

## 21cm Absorption Lines at High Redshift from Intervening Galaxies

F. H. Briggs

*Kapteyn Astronomical Institute, 9700 AV Groningen, The Netherlands*

**Abstract.** Radio absorption line observations of neutral hydrogen gas against extended radio sources offers the means to measure sizes and kinematics in intervening galaxies at all redshifts up to the maximum redshift where radio galaxies are detected. Such observations can therefore trace the evolution of galaxies at redshifts  $z \gtrsim 2$  where the damped Lyman- $\alpha$  statistics indicate that the mass in neutral gas exceeded the mass in stars.

### 1. Introduction

Theoretical simulations, which are successfully tuned to produce the  $z = 0$  large scale structure starting from initial conditions that are consistent with the level of fluctuation in the microwave background, predict mass distribution functions for protogalaxies through cosmic time. These simulations, which are based on the gravitational collapse of structures within Cold Dark Matter and Cosmological Constant dominated Universes, demonstrate a hierarchical clustering that shows galaxies forming by the dissipationless merging of low mass dark matter mini-halos and the subsequent accretion of condensing, dissipational gas (cf. White & Frenk 1991, Kauffman 1996, Ma et al 1997). In these scenarios, the more massive galaxies “form late,” having been built up over the age of the Universe.

The postponement of the assembly of massive galaxies in the CDM models is somewhat at odds with observations showing powerful radio galaxies at redshift above  $z = 5$  (van Breugel et al 1999) and kinematic evidence for large gaseous disks in well-formed potentials at  $z \approx 2.5$  (Prochaska & Wolfe 1999). A crucial test of the formation ideas will be to measure the sizes of galaxies and their total dynamical masses as a function of redshift in order to define the time sequence of galaxy formation.

### 2. Evolution of global properties $z = 4$ to $z = 0$

A number of indicators trace global properties of the Universe through the epoch of most vigorous assembly of galaxies. Fig. 1 shows four of these plotted as a function of redshift. (1) The star formation rate SFR density computed for color-selected, star forming galaxies (cf Madau et al 1996, Calzetti and Heckman 1999) shows a steep rise with redshift to  $z \approx 1$  with a modest decline at higher redshifts. More recent observational evidence (Steidel et al 1999) favors a flat SFR density above  $z = 1$  to at least  $z = 4$ , once corrections have been made

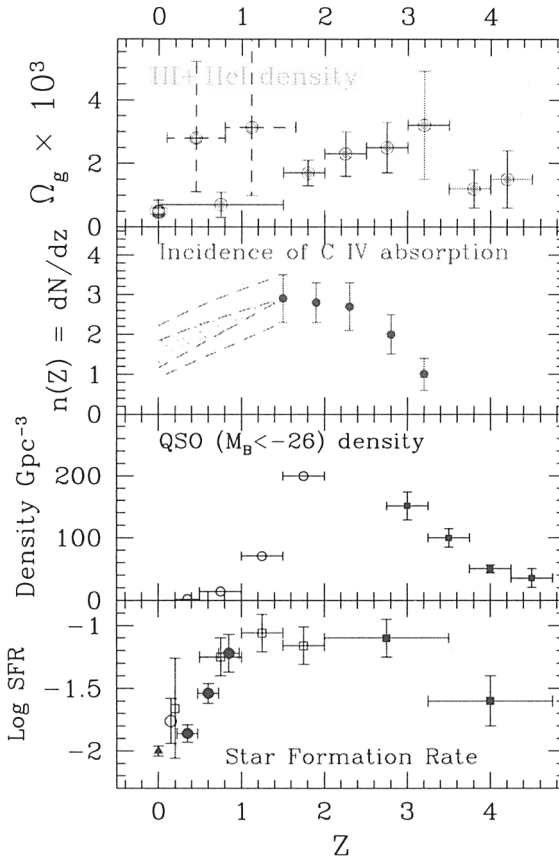


Figure 1. Cosmological density of neutral gas, incidence of CIV absorption, comoving density of luminous QSOs, and mean star formation rate as a function of redshift. *Top panel.* Mean cosmological density of neutral gas,  $\Omega_g$ , normalized to the critical density (Storrie-Lombardi et al 1996; Lanzetta et al 1995, Zwaan et al 1997 ( $z = 0$ ), Turnshek 1998: dashed error bars) *Upper middle panel.* Number of CIV metal-line absorption systems per unit redshift,  $n(z)$  (Steidel 1990). Hatched areas indicate the range ( $0 < q_0 < 1/2$ ) for unevolving cross sections since  $z = 1.5$ , beyond which redshift CIV can be measured with ground-based telescopes. *Lower middle panel.* Comoving density of optically selected QSOs: filled squares from Schmidt et al 1994; open circles from Hewitt et al 1993).  $H_0 = 50 \text{ km s}^{-1} \text{ Mpc}^{-1}$ ,  $q_0 = 1/2$  *Bottom panel.* Comoving star formation rate density  $M_{\odot} \text{ yr}^{-1} \text{ Mpc}^{-3}$  from Madau (1998) and references therein.

for extinction. (2) The comoving space density of luminous optically selected quasars reaches a maximum at  $z \approx 2$ , implying that mass is being redistributed within the evolving galaxies to efficiently feed nuclear activity. (3) Studies of absorption lines against the ultraviolet continua of bright high redshift quasars provide probes of the comoving density of neutral gas, through studies of the damped Lyman- $\alpha$  DLa line of HI (Wolfe et al 1986), as well as (4) the ionized galaxy halo gas that is sensed in CIV (Steidel 1990). Quasar absorption lines well suited to the study of normal galaxies, since they are not biased toward the luminous objects at the peak of the luminosity function for a chosen redshift, but rather the quasar absorption lines provide a democratic selection of the common, gas rich objects that represent the less rapidly evolving protogalaxies that are contain the bulk of the baryons destined to eventually be locked into galaxies at  $z = 0$ .

The DLa lines are especially relevant to the discussion here, since the quantities of cool neutral gas sensed in these high redshift absorbers exceeds the local HI comoving density  $\Omega_g(z = 0)$  by a factor of at least five (Wolfe et al 1995, Lanzetta 1995), and the HI is a viable target for radio studies in the 21cm line of HI, since the DLa class comprises neutral gas layers with  $H^0$  column densities above  $2 \times 10^{20} \text{cm}^{-2}$ .

The past two decades have seen extensive synthesis mapping of the detailed gas kinematics of nearby spiral galaxies in the 21cm emission line. In this application, the HI is a highly diagnostic tracer of the galactic potential. Even the integral spectra obtained with single-dish telescopes yields a "mass indicator" by measurement of the profile width. The settled and quiescent nature of neutral gas layers makes them a more reliable tracer of gravitational potentials than emission line gas in HII regions around star forming regions, where stellar winds and expanding shock fronts compete with gravitation in determining the gas kinematics.

An interesting comparison can be made between the observed sizes of the high- $z$  star forming galaxies (Giavalisco et al 1996a) and the interception cross-sections for uv absorption by different ions (cf. Steidel 1993). The Lyman-break color-selection technique for identifying the star forming galaxies produces candidates with a density on the sky of  $\sim 1 \text{ arcmin}^{-2}$  for objects with redshifts predominantly in the range  $2.6 \leq z \leq 3.4$  (Steidel et al 1998). The comoving density of  $L \geq L_*$  galaxy "sites," computed for this redshift range, amounts to  $\sim 2 \text{ arcmin}^{-2}$  (for a cosmological model with  $\Omega_o = 0.2$ ). Fig. 2 shows the cross section for absorption lines that every  $L_*$  galaxy site would necessarily present, if ordinary galaxies are to explain the observed incidence of absorption lines. Thus, absorption line statistics indicate  $\sim 2$  times the absorption cross sections shown in Fig. 2 for every Lyman-break galaxy. At low and intermediate redshifts ( $z < 1$ ), the association of the metal line absorbers with the outer regions of galaxies has been well established for the MgII class of absorber by observation of galaxies close to the lines of sight to the background quasars (Le Brun et al 1993). The CIV selected systems are consistent with galaxy halo cloud properties (Petitjean & Bergeron 1994, Guillemin & Bergeron 1997), and ionized high velocity cloud (HVC) analogs for the CIV cloud population exist in the halo of the Milky Way (Sembach et al 1999). A few of the DLa absorbers are also identified with galaxies at intermediate redshift (Steidel et al 1994, Steidel

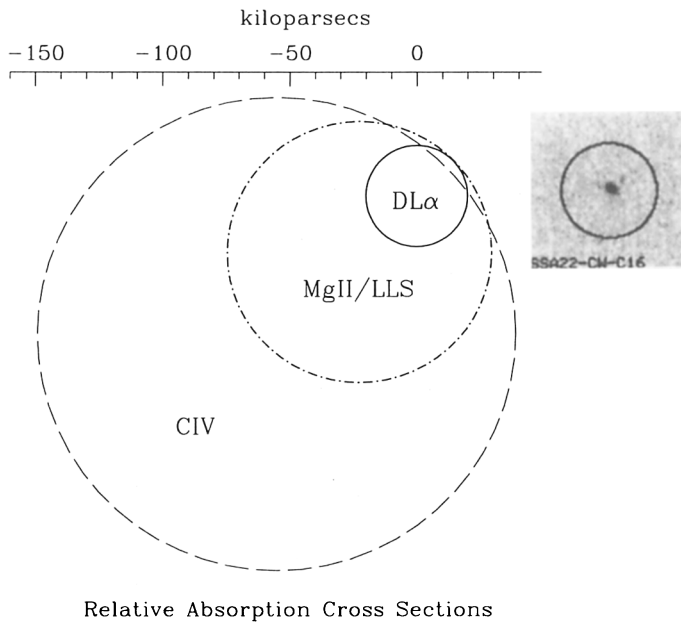


Figure 2. Comparison of quasar absorption-line cross sections for CIV, MgII-Lyman Limit, and damped Lyman- $\alpha$  lines with the physical size of the optical emission from a color-selected galaxy at  $z \approx 3$  *top right* (Giavalisco et al 1996). The  $z \approx 3$  galaxy is centered in a  $5''$  diameter circle that subtends 37.5 kpc ( $H_o = 75 \text{ km s}^{-1} \text{ Mpc}^{-1}$ ,  $\Omega = 0.2$ ).

et al 1995). The optical identification of the DLa systems has gone more slowly than for the MgII, for example, because DLa absorbers are rarer (as indicated by the relative cross sections), and the majority of the surveys for DLa systems have been conducted with ground-based telescopes, which find  $z > 1.7$  systems that are difficult to associate with galaxies. Curiously, some of the studies of the lowest redshift DLa absorbers have failed to provide any optical identification to sensitive limits (Rao & Turnshek 1998).

The overall implication of a comparison between the physical sizes of the Lyman-break galaxies and the absorption-line cross sections for the high- $z$  Universe is that there is a substantial population of metal-enriched gaseous objects, possibly accompanied by a tiny pocket of stellar emission, that can well go unnoticed in deep optical images. The nature of these invisible absorbers remains a puzzle.

### 3. Sizes and kinematics of the DLa Clouds

Fortunately, definitive measurements can be obtained through high spatial resolution observations of absorption against extended background radio sources. The statistics for damped Lyman- $\alpha$  absorbers show that roughly half of the radio sources with redshift greater than 4 will lie behind DLa absorbing layers.

Considerable progress in assessing the extent and kinematics of the DLa class of quasar absorption line system can be made with the current generation of radio telescopes, including GMRT, WSRT and the EVN VLBI network, equipped with broad band UHF receivers. The technique of course requires background radio quasars or high redshift radio galaxies with extended radio continuum emission, so effort needs to be invested in surveys to find redshifted 21cm line absorption against these types of sources. These surveys can either key on optical spectroscopy of the quasars to find DLa systems for subsequent inspection in the 21cm line, or they can make blind spectral surveys in the 21cm line directly, once the new wideband spectrometers that are being constructed for at Westerbork and the new Green Bank Telescope are completed. Then radio interferometers such as GMRT with suitable angular resolution at the redshifted 21cm line frequency must be used to map the absorption against the extended background source. Ideally, interferometer baselines should extend to a few hundred kilometers – shorter than is typically associated with VLBI techniques, but longer than the present the VLA and GMRT baselines. The shorter spacings in the European VLBI Network and the MERLIN baselines would form an excellent basis for these experiments, although considerable effort will be required to observe at the interference riddled frequencies outside the protected radio astronomy bands.

Fig. 3 shows an example of how these experiments might work. The top panel shows contours for the radio source 3C196. Brown and Mitchell (1983) discovered a 21cm line in absorption at  $z = 0.437$  against this source in a blind spectral survey. The object has been the target of intensive optical and UV spectroscopy (summarized by Cohen et al 1996), as well as HST imaging to identify the the intervening galaxy responsible for the absorption (Cohen et al 1996, Ridgway and Stockton 1997). Fig. 3 includes a dashed ellipse in the top panel to indicate the approximate extent and orientation of the galaxy identification.

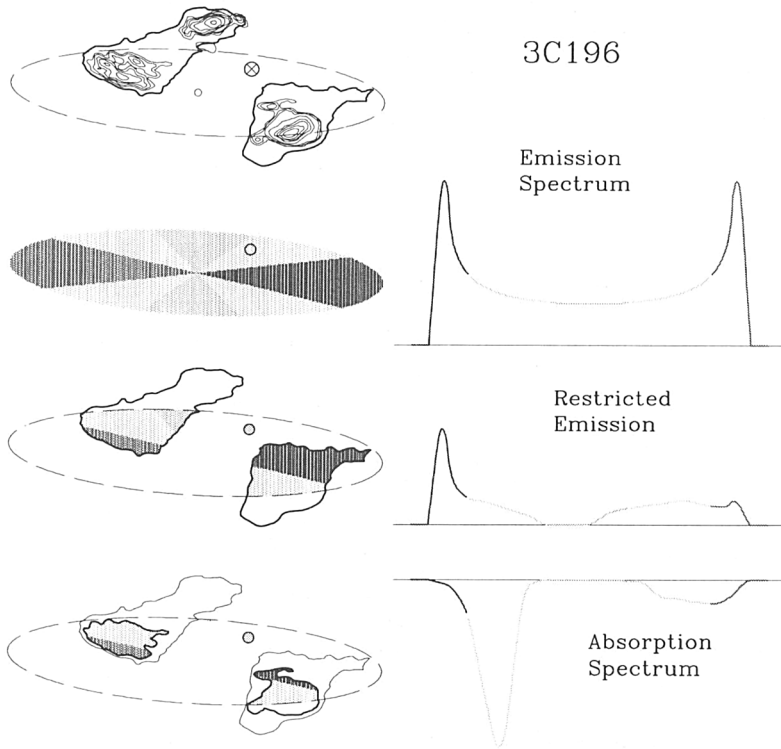


Figure 3. Absorption by an intervening disk galaxy against an extended background radio quasar. *Top*: Contours of radio continuum emission (Lonsdale 1984 with the outer radio contour taken from the map of Oren as shown by Cohen et al 1996). *Upper middle*: The velocity field of and emission profile expected for disk galaxy. *Lower middle*: A spectrum that has been restricted to gas lying in front of background continuum; in principle, sensitive mapping could measure the distribution and kinematics for these clouds in absorption across the face of the radio source. *Bottom*: The integral absorption spectrum obtained by observing this source with a low angular resolution telescope.

The second panel from the top in Fig. 3 illustrates the 21cm line emission spectrum typical of nearby HI-rich disk galaxies, observed by a low resolution (“single-dish”) beam that does not resolve the gaseous structure in the galaxy. The rotation of a galaxy with a flat rotation curve produces the velocity field shown to the left of the spectrum

For disk systems observed in absorption, the information accessible to the observer is less, since we can only hope to ever learn about the gas opacity and kinematics for regions that fall in front of background continuum. This restricts our knowledge to zones outlined in the third panel of Fig. 3. The “restricted emission” spectrum is drawn to illustrate what fraction of the galaxies gas content might be sensed by a sensitive synthesis mapping observation. A comparison to the total gas content in the upper spectrum suggests that much of the important information (velocity spread, for example) would be measured by a synthesis map of the absorption against background source.

The single-dish spectrum of the absorption lines observed for an object like 3C196 is weighted by the regions where the background continuum has the highest brightness. As shown in the lower panel, this weighting emphasizes the bright spots in the radio lobes. Clearly sensitive mapping will better recover the information lost in the integral spectrum produced by a low angular resolution observation. A preliminary look at recent observations of the  $z = 0.437$  absorber in 3C196 can be found in de Bruyn et al (1997).

#### 4. Conclusion

Radio mapping in the redshifted HI line with modest spatial resolution radio interferometers promises to resolve basic questions about how galaxies assemble and evolve. By observing the cool neutral gas that traces gravitational potential wells of forming galaxies, the 21cm line provides not only a measure of the neutral gas content of the Universe over cosmic time scales but also a method to weigh the dark matter halos. The new GMRT will play an important role in deciphering the time-sequence of galaxy formation.

#### References

- Brown, R.L., & Mitchell, K.J. 1983, *ApJ*, 264, 87  
Calzetti, D., & Heckman, T.M. 1999, *ApJ*, 519, 27  
Cohen, R.D., Beaver, E.A., Diplas, A., et al. 1996, *ApJ*, 456, 132  
de Bruyn, A.G., Briggs, F.H., & Vermeulen, R.C. 1997,  
<http://www.nfra.nl/nfra/newsletter/1997-1/index.htm>  
Giavalisco, M., Steidel, C.C., & Macchetto, F.D. 1996, *ApJ*, 470, 189  
Guillemin, P., & Bergeron, J. 1997, *A&A*, 328, 499  
Hewett, P.C., Foltz, C.B., & Chaffee, F.H. 1993, *ApJ*, 406, L43  
Kauffmann, G. 1996, *MNRAS*, 281, 475  
Lanzetta, K.L., Wolfe, A.M., & Turnshek, D.A. 1995, *ApJ*, 440, 435  
Le Brun, J., Bergeron, J., Boisse, P., & Christian, C. 1993, *A&A*, 279, 33  
Lonsdale, C.J. 1984, *MNRAS*, 208, 545

- Ma, C.-P., et al. 1997, *ApJ*, 440, L1
- Madau, P., et al. A. 1996, *MNRAS*, 283, 1388
- Madau, P. 1998, in *The Hubble Deep Field*, eds. M. Livio, S.M. Fall, & P. Madau, *STScI Symposium Series*, astro-ph/9709147
- Petitjean, P., & Bergeron, J. 1994, *A&A*, 283, 759
- Prochaska, J.X., & Wolfe, A.M. 1997 *ApJ*, 487, 73
- Ridgway, S.E., & Stockton, A. 1997, *AJ*, 114, 511
- Rao, S.M., & Turnshek, D.A. 1998, *ApJ*, 500, L115
- Schmidt, M. Schneider, D.P., & Gunn, J.E. 1994, *AJ*, 107, 1245
- Sembach, K.R., Savage, B.D., Lu, L., & Murphy, E.M. 1999, *ApJ*, 515, 108
- Steidel, C.C. 1990, *ApJS*, 72, 1
- Steidel, C.C. 1993, in *The Environment and Evolution of Galaxies*, eds. J.M. Shull & H.A. Thronson, *Kluwer Academic Publ.*, p. 263
- Steidel, C.C., Pettini, M., Dickinson, M., & Persson, S.E. 1994, *AJ*, 108, 2046
- Steidel, C.C., Bowen, D.V., Blades, J.C., & Dickinson, M. 1995, *ApJ*, 440, L45
- Steidel, C.C., et al. 1998, in *The Young Universe*, eds. d'Odorico, Fontana, and Giallongo, *ASP Conference Series*.
- Steidel, C.C., Adelberger, K.L., Giavalisco, M., & Pettini, M. 1999, *ApJ*, 519, 1
- Storrie-Lombardi, L.J., McMahon, R.G., & Irwin, M.J. 1996, *MNRAS*, L79
- Turnshek, D.A. 1998, in *Structure and Evolution of the Intergalactic Medium from QSO Absorption Line Systems*, eds. Petitjean, P., & Charlot, S., p. 263
- van Breugel, W., et al. 1999, *ApJ*, 518, L61
- Wolfe, A.M., Turnshek, D.A., Smith, H.E., Cohen, R.D. 1986, *ApJS*, 61, 249
- Wolfe, A.M., Lanzetta, K.M., Foltz, C.B., & Chaffee, F.H. 1995, *ApJ*, 454, 698
- Zwaan, M., Briggs, F., Sprayberry, D., & Sorar, E. 1997, *ApJ*, 490, 173